ARTICLE

doi:10.1038/nature21416

Aboriginal mitogenomes reveal 50,000 years of regionalism in Australia

Ray Tobler[1]*, Adam Rohrlach[2,3]*, Julien Soubrier[1,4], Pere Bover[1], Bastien Llamas[1], Jonathan Tuke[2,3], Nigel Bean[2,3], Ali Abdullah-Highfold[5], Shane Agius[5], Amy O'Donoghue[5], Isabel O'Loughlin[5], Peter Sutton[5,6], Fran Zilio[5], Keryn Walshe[5], Alan N. Williams[7], Chris S.M. Turney[7], Matthew Williams[1,8], Stephen M. Richards[1], Robert J. Mitchell[9], Emma Kowal[10], John R. Stephen[11], Lesley Williams[12], Wolfgang Haak[1,13]§ & Alan Cooper[1,14]§

Aboriginal Australians represent one of the longest continuous cultural complexes known. Archaeological evidence indicates that Australia and New Guinea were initially settled approximately 50 thousand years ago (ka); however, little is known about the processes underlying the enormous linguistic and phenotypic diversity within Australia. Here we report 111 mitochondrial genomes (mitogenomes) from historical Aboriginal Australian hair samples, whose origins enable us to reconstruct Australian phylogeographic history before European settlement. Marked geographic patterns and deep splits across the major mitochondrial haplogroups imply that the settlement of Australia comprised a single, rapid migration along the east and west coasts that reached southern Australia by 49–45 ka. After continent-wide colonization, strong regional patterns developed and these have survived despite substantial climatic and cultural change during the late Pleistocene and Holocene epochs. Remarkably, we find evidence for the continuous presence of populations in discrete geographic areas dating back to around 50 ka, in agreement with the notable Aboriginal Australian cultural attachment to their country.

At the time of initial human colonization (around 50 ka)[1,2], Australia and New Guinea were connected as a single landmass (termed Sahul) that remained contiguous until separated by rising sea levels around 9 ka (ref. 3). Despite this, the initial Sahul colonists appear to have rapidly diverged into distinct New Guinean and Australian populations, with limited signs of subsequent gene flow[4–12]—although genetic data remains sparse. Little is known about the post-colonization diversification of Australian lineages or the effects of major environmental and cultural changes over the last 50 thousand years (kyr). Palaeoclimatically, these include continental-scale aridification and cooling of Australia during the Last Glacial Maximum (21 ± 3 ka), warming in the early Holocene (9–6 ka), and intensification of the El Niño/Southern Oscillation during the mid-to-late Holocene (4–2 ka)[13,14]. Substantial changes in the cultural record are not observed until the terminal Pleistocene and Holocene, and include the formation of the Panaramittee art style, the spread of the Pama–Nyungan group of languages across most of the continent, and the increase in diversity and complexity of technology and resource exploitation[15,16]. Aboriginal history is inextricably interwoven with the Australian landscape and is culturally expressed through the central importance of kin group attachment to 'country', and further reinforced through Songlines and Dreaming narratives[17]. Close relationships to the landscape are likely to have played an important role in surviving the extreme environmental changes of late Pleistocene Australia.

Reconstructing the genetic history of Aboriginal Australia is greatly complicated by past government policies of enforced population relocation and child removal that have eroded much of the physical connection between groups and geography in modern Australia. However, a unique opportunity is provided by a remarkable set of hair samples and detailed ethnographic metadata collected with permission from more than 5,000 Aboriginal Australians during expeditions run by the Board for Anthropological Research (BAR) from the University of Adelaide between the 1920s and 1970s (Supplementary Information). The extensive genealogical and geographical information collected with the samples allows detailed reconstruction of the genetic and historical relationships between Aboriginal Australian groups before the effects of European colonization.

Dataset

We obtained informed consent from hair donors or their families (Supplementary Information) to perform genetic analyses and sequenced complete mitogenomes from hair samples of 111 individuals across three different Aboriginal communities (Point Pearce, South Australia; Cherbourg, Queensland; Koonibba, South Australia; Supplementary Information). Using the genealogical and cultural metadata, we traced the geographic origin of each individual (referred to as BAR samples) as far back as possible along the ancestral maternal lineage. The resulting broad geographic range is shown in Extended Data Fig. 1. We identified 54 unique mtDNA haplotypes, which fell into the five major mitochondrial haplogroups S, O, M, P and R that have been described previously for Aboriginal Australia[9,10,12] (Supplementary Information). Phylogenetic relationships were

[1]Australian Centre for Ancient DNA, School of Biological Sciences, The University of Adelaide, Adelaide, South Australia 5005, Australia. [2]School of Mathematical Sciences, The University of Adelaide, Adelaide, South Australia 5005, Australia. [3]ARC Centre of Excellence for Mathematical and Statistical Frontiers, The University of Adelaide, Adelaide, South Australia 5005, Australia. [4]Genetics and Molecular Pathology, SA Pathology, Adelaide, South Australia 5000, Australia. [5]South Australian Museum, Adelaide, South Australia 5005, Australia. [6]School of Biological Sciences, The University of Adelaide, Adelaide, South Australia 5005, Australia. [7]Palaeontology, Geobiology and Earth Archives Research Centre, and Climate Change Research Centre, School of Biological, Earth and Environmental Sciences, University of New South Wales, Sydney, New South Wales 2052, Australia. [8]School of Archaeology and Anthropology, College of Arts and Social Sciences, Australian National University, Canberra, Australian Capital Territory 0200, Australia. [9]Department of Biochemistry and Genetics, La Trobe University, Melbourne, Victoria 3086, Australia. [10]Alfred Deakin Institute, Deakin University, Melbourne, Victoria 3125, Australia. [11]Australian Genome Research Facility, The Waite Research Precinct, Adelaide, South Australia 5064, Australia. [12]Community Elder and Cultural Advisor, Cherbourg, Queensland, Australia. [13]Department of Archeogenetics, Max Planck Institute for the Science of Human History, 07745 Jena, Germany. [14]Environment Institute, The University of Adelaide, Adelaide, South Australia 5005, Australia.
*These authors contributed equally to this work.
§These authors jointly supervised this work.

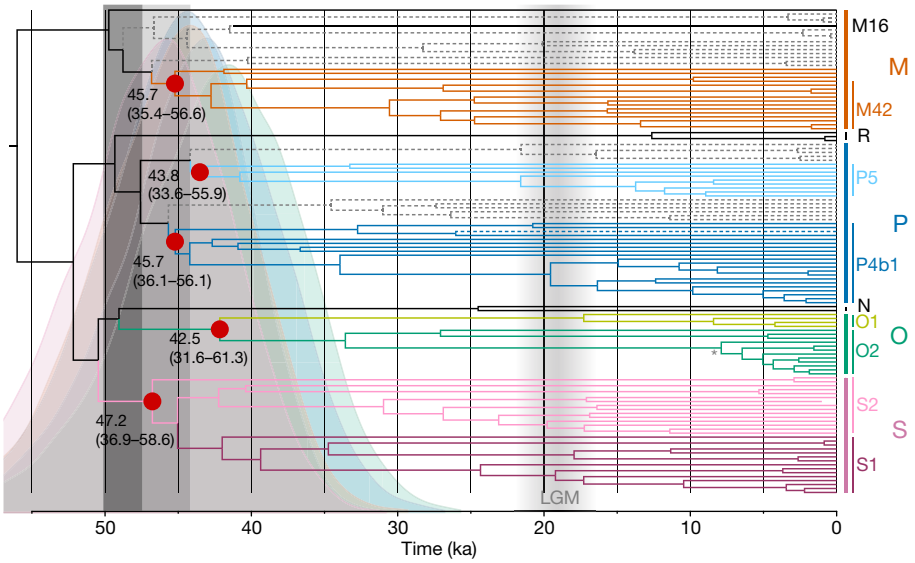

Figure 1 | Australian mtDNA phylogeny. Phylogenetic analysis of Aboriginal Australian and Melanesian (dashed grey lines) mitogenomes using BEAST[31], showing the four major haplogroups detected in Australia (in colour), along with other Aboriginal Australian lineages not used in dating analyses (solid black lines). The age of the most recent common ancestor (TMRCA) and 95% highest posterior density intervals were calculated for each Aboriginal-Australian-only clade (red dots) using human mitochondrial evolutionary rates calibrated with Palaeolithic European and Asian mitogenomes[18,32] to minimize the effects of rate temporal dependency[33,34] (see Methods). The posterior distributions for each TMRCA are shown behind the phylogeny, in matching colours. The dark grey box represents the initial colonization of Australia indicated by archaeological evidence at 48.8 ± 1.3 ka (see Methods). The light grey box indicates the period when mitochondrial lineages were still sorting into Australia or New Guinea/Melanesia, which occurred during the initial colonization of Sahul. Genetic divergences during this time (for example, between M16 and M42, or O and N) might have occurred outside Australia, and were excluded from TMRCA calculations. The short branch length of an ancient S2 sequence[14] reflects the radiocarbon-dated age of the specimen. The early Holocene diversification of lineages within haplogroup O2 is indicated with an asterisk. LGM, Last Glacial Maximum.

analysed with other full mtDNA haplotypes from Aboriginal Australians and Melanesians (44 and 25 samples, respectively, 123 unique mtDNA lineages in total).

Dating the colonization of Sahul

The timing of human arrival in Australia was estimated using the age of the most recent common ancestor (TMRCA) for the different Australian-only haplogroups, calculated using a molecular clock with substitution rates calibrated with ancient European and Asian mitogenomes[18]. Although these TMRCA values are likely to be minimal estimates given the limited sampling, they group in a narrow window of time from approximately 43–47 ka (Fig. 1 and Extended Data Figs 2, 3), consistent with previous studies (Supplementary Information). To examine the accuracy of this molecular age estimate we re-analysed a comprehensive suite of radiocarbon and optically stimulated luminescence ages from early archaeological sites across Sahul using currently available calibration datasets[19] and the phase function in OxCal 4.2.4. The resulting independent estimate for initial colonization of Sahul, 48.8 ± 1.3 ka, is a close match to the genetic age estimates (Fig. 1 and Supplementary Table 4). Indeed, the basal splits between haplogroups O, S and N13, P and R, M16 and M42 (Fig. 1) might reflect the initial within-Australia events, around 50 ka. However, we have taken a conservative approach and assumed these reflect lineages present in the initial population colonizing Sahul, as suggested by the presence of basal sister clades of Melanesian and Aboriginal Australian lineages within haplogroups M and P (Fig. 1).

Aboriginal Australian phylogeography

Phylogenetic analysis of all Aboriginal Australian samples with reliable geographical information (74 BAR samples and two from previous mtDNA studies[8,14], 76 lineages in total; see Methods), revealed large-scale phylogeographic patterns for each major haplogroup (Fig. 2). For example, none of the haplogroup O lineages were found in eastern Australia, which was dominated by haplogroups P, S and M42a. Within the two main Australian P-clades (based around P5 and P4b1) there was a clear split between northeastern and Riverine/South Australia (Fig. 2). Similar patterns are observed in the other major haplogroups, indicating that Aboriginal Australian mitochondrial lineages have undergone limited amounts of dispersal over time, and related lineages are grouped geographically. Furthermore, the basal lineages within each major haplogroup were mostly in northern Australia, presumably reflecting early divergences as members of the founding populations remained while others moved south where more derived lineages were observed. Together with the deep divergences among the mtDNA lineages, these results suggest that populations were structured by the initial major population movements following colonization around 50 ka (Fig. 1).

To verify that the small sample sizes are not biasing the phylogeographic patterns, we used a novel correlation test based on the results of a multiple correspondence analysis to examine the 76 mtDNA lineages with reliable provenance. This method is a generalization, for individual haplotypes, of the principal component analysis used for population genetic analyses of diploid genotypes. The major axes of variation among the pooled haplotype data are determined and then used to test for significant correlations with supplementary variables of interest. The test showed strong phylogeographic clustering among Aboriginal Australian mtDNA lineages, and a significant correlation between the phylogenetic structure between and within each haplogroup and both the latitudinal and longitudinal origin of the samples (Table 1 and Extended Data Table 1). As a second test for relative geographic structure, we applied a Mantel test to find correlations between pairwise distances for individuals calculated from geographic and genetic coordinates (from the multiple correspondence analysis). We also found significant correlations between these distances, both within and between haplogroups, indicating (geographically) neighbouring individuals were closely related genetically (Table 1 and Extended Data Table 1). These findings confirm that there was strong phylogeographic clustering among Aboriginal Australian mtDNA lineages before European colonization, differentiated along latitudinal and longitudinal gradients, indicating that there were very limited amounts of geographic

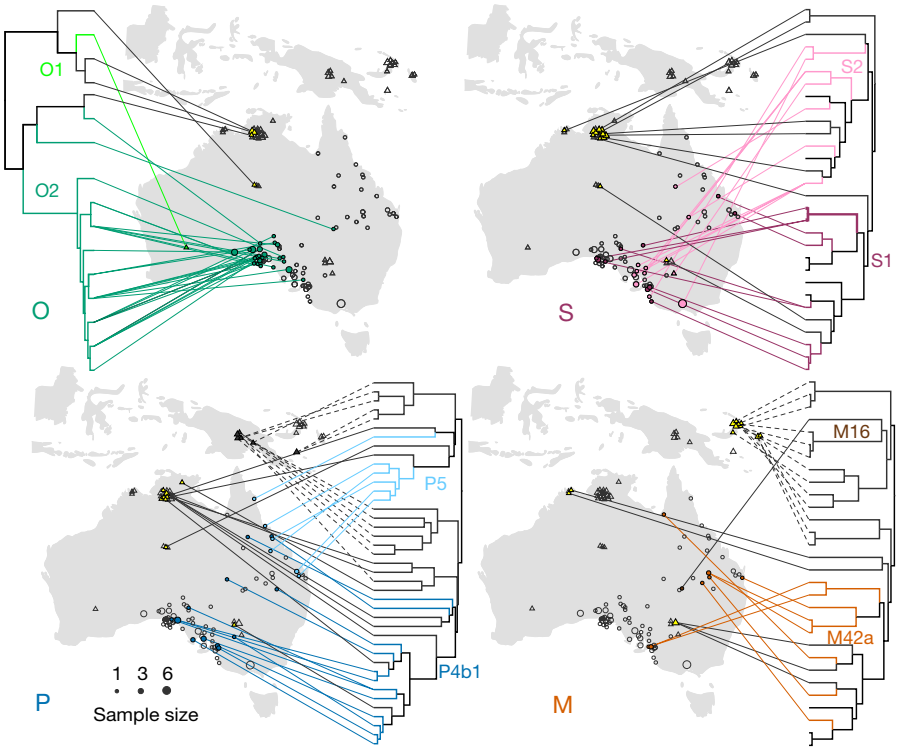

Figure 2 | Australian mtDNA phylogeography. Phylogeographic distributions of Aboriginal Australian mitogenome haplotypes, grouped into the four major haplogroups O, S, P and M with timescales calculated using an ancient-DNA-calibrated molecular clock (see Methods). Lineages from samples in the current study (circles) are shown at the location of the oldest known maternal ancestor recorded in genealogical and geographic data, generally before the effects of European colonization. Triangles represent data from modern samples reported in previous studies. The size of the symbols reflects the number of identical haplotypes as indicated in the figure. Identical sequences from the same location were pruned, whereas those from multiple locations were only used where they could not be explained through genealogical records. Coloured circles and lines represent haplotypes with known geographical provenance, with colours matching the cluster assignments of the multiple correspondence analysis (Supplementary Table 3), whereas grey (empty) circles represent the geographic distribution of samples not falling within each specific haplogroup. Previously published haplotypes that lack detailed geographic data histories are shown with yellow triangles (and black lines) for each haplogroup, whereas those with no associated locations are shown on the tree as black branches alone. Map data was sourced from the Oak Ridge National Laboratory Distributed Active Archive Center (https://webmap.ornl.gov/wcsdown/wcsdown.jsp?dg_id=10003_1).

dispersal given the long time periods involved. Similarly, an additional set of Aboriginal Australian mtDNA genomes recently generated as part of a genomic study[12] show a concordant phylogeographic distribution to the patterns in our data (Extended Data Fig. 4). However, these sequences are not available and the samples lack information about pre-European distributions, complicating historical analysis.

Migratory patterns and regionalism within Australia

The phylogeographic distribution of the major Aboriginal haplogroups are consistent with coastal colonization models of Australia[20,21] where the initial Sahul colonizers spread across northern Australia, and then south along the east (haplogroups P, S, M42a) and west (haplogroups O, R) coasts in parallel clockwise and counter-clockwise movements (Fig. 3). The disjunction between haplogroups O and S in central southern Australia (Fig. 2) potentially reflects a meeting of the two movements. Limited genetic surveys in Tasmania are consistent with this model, because haplogroups P, S and M were detected, but not haplogroup O or R (ref. 22). A major migration corridor is also apparent between northeastern and southern Australia, potentially along the Murray–Darling River[23].

The 49–45 ka age range recently reported from Warratyi rock shelter[24], Flinders Ranges, South Australia is close in age to the earliest sites reported from northern Australia[1]. To similarly constrain the timing of human arrival in the far southwest of Australia, we re-examined the multi-dated sequence of Devil's Lair, southwestern Australia (Extended Data Fig. 5) along with continental-wide earliest occupation ages (Supplementary Table 4). The resulting age estimate (47.8 ± 1.5 ka), together with multiple early occupation sites across southern Australia (Fig. 3 and Extended Data Fig. 6) suggest the initial expansion around Australia was very rapid, perhaps taking only a few thousand years. The initial human colonization considerably preceded the extinction of the last megafauna[25], as indicated by the presence of the Diprotodont *Zygomaturus* at 42 ka just south of the Flinders Ranges[26], and this temporal overlap is similar to the pattern recently reported for South America[27].

The marked population structure of deeply diverged Aboriginal Australian mitogenomes appears to date back to the original arrival of people on the Australian part of Sahul. These patterns are surprising given the pronounced environmental changes that have occurred since

Table 1 | Australian phylogeography test results

Haplogroup	O	S	M (without M16)	P
Longitude	−0.6395 (0.0629)*	0.3351 (0.0016)***	0.642 (0.0929)*	0.7796 (0.0002)***
Latitude	0.5010 (0.0083)***	0.5977 (0.0006)***	0.8560 (0.0055)***	0.8690 (4×10^{-6})***
Mantel test	0.3352 (0.0176)**	0.2695 (0.0374)**	0.3273 (0.0953)*	0.4488 (3×10^{-6})***

Tests based on multiple correspondence analysis of phylogeographic structure within the major Aboriginal Australian haplogroups reveal significant correlations with latitude and longitude, implying lineages are likely to be found in certain geographic locations. Mantel tests confirm the lineages are grouped geographically on the landscape, implying that neighbouring individuals are expected to share common ancestry (see Methods). For each haplogroup, the correlation coefficient is given for the dimension with the most significant correlation in the case of longitude and latitude, along with the *P* value in brackets (*$P < 0.1$; **$P < 0.05$; ***$P < 0.01$). Although not every principal dimension is significantly correlated with geography, we would not expect that this is the only driver for lineage distribution.

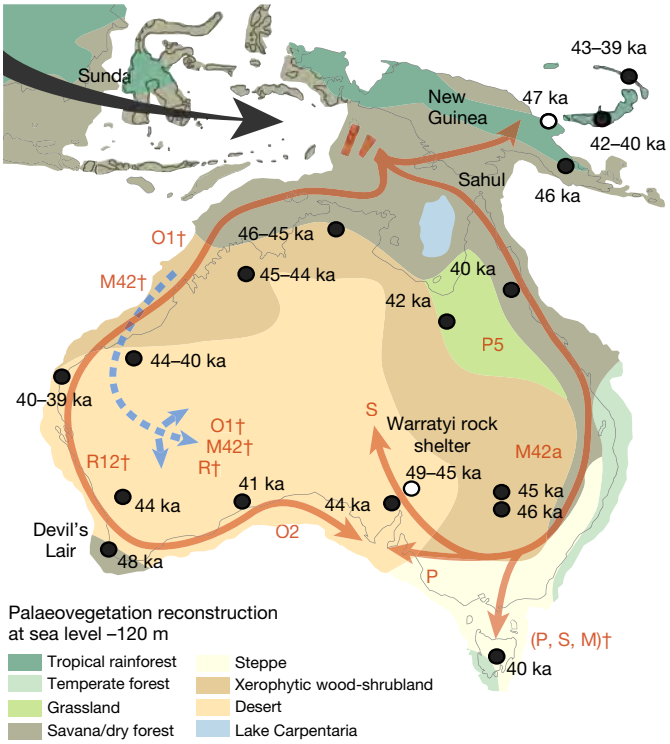

Figure 3 | The peopling of Australia. Model of the peopling of Australia combining genetic and archaeological data, showing approximate, and stylised, coastal movements of haplogroups O and R (west) and P, S, and M (east). The inferred movement of S into the interior is influenced by the path of a recent study on water sources and human movement[21]. Data from other studies where pre-European distributions are unclear are indicated with a dagger (†), and include a potential late-glacial movement into the western central desert region (blue dashed arrows; see Methods). Early archaeological sites in Australia and New Guinea (black dots) are given with mean ages for earliest occupation of sites in each region (Supplementary Table 4). Insufficient data were available for sites with white dots, which were not used in the age model for the initial Sahul colonization date but provide independent age controls. Ages in southwestern and south central Australia, at Devil's Lair (49–46 ka) and Warratyi rock shelter (49–45 ka), suggest that the overall population movements were rapid and that the coastal regions of Australia were colonized within a few thousand years. Approximate late Pleistocene vegetation reconstructions are shown (from ref. 35). The map was adapted from the figure in ref. 36, originally constructed by J.S.

initial colonization. The most extreme example of this is the widespread aridification and cooling of the Last Glacial Maximum, during which archaeological models suggest pronounced geographic contraction of populations and abandonment of large parts of the continent[28]. The diversity and grouping of Aboriginal Australian mitogenome data indicate that Aboriginal Australian populations survived these changes without large-scale movements, although there is potential evidence for a late-glacial (approximately 15 ka) re-expansion into the Western central desert (Extended Data Fig. 4 and Supplementary Information). Notably, both the diversity of mitochondrial lineages and population size estimates during this time period do not suggest severe population bottlenecks (Fig. 1 and Extended Data Fig. 7), indicating that many populations survived in local refugia that may have been cryptic to the archaeological record[29].

Holocene intensification

The rapid diversification of derived haplotypes within haplogroup O2 is indicative of a population expansion around 7 ka in southern Australia (Fig. 1), but this is the only obvious genetic signal that coincides with the mid-Holocene climatic optimum (9–6 ka) and the increasing accessibility of the arid interior to hunter–gatherer groups[13,15]. The above suggests that the extensive cultural changes evident during the Holocene, including the establishment of Panaramittee rock art, spread of the Pama–Nyungan languages, adoption of complex and diversified technologies (for example, seed grinding, wooden toolkits), advanced food-processing techniques (of, for example, *Macrozamia* plants), and greater reliance on marine resources, may have been the result of demographic change and/or cultural transmission, rather than population movement or replacement[15]. In this regard, recent archaeological models propose that rapid demographic growth during the Holocene led to reduced mobility and a consequent greater investment in technology[15]. It is also possible that some cultural changes were entirely male-mediated, and therefore not apparent in mtDNA data. Recent genomic data from modern Aboriginal Australians has been used to tentatively link the spread of the Pama–Nyungan languages to an early Holocene population expansion in northeast Australia, and limited gene flow to the rest of Australia[12]. However, the strength of the genetic signal for both the population expansion and movement remains ambiguous at best (Supplementary Information).

Discussion

The long-standing and diverse phylogeographic patterns documented here are remarkable given the timescale involved, and raise the possibility that the central cultural attachment of Aboriginal Australians to 'country' may reflect the continuous presence of populations in discrete geographic areas for up to 50 kyr. The very limited geographical movement of populations over time is consistent with observations of nomadic sedentism in recent Aboriginal Australian societies, where ranging was anchored in localized, collective and stable land/language ownership units, and occurred within a broad environmental region[17] (Supplementary Information). This form of subsistence (and territoriality) might also explain the notable lack of exchange between New Guinea and Australian mitochondrial lineages, despite a land bridge between the two until about 9 ka. Overall, these patterns are similar to recent reports of marked mitochondrial phylogeography in early South American populations[30], and raise the possibility that hunter–gatherer groups were capable of exhibiting pronounced regionalism, or at least female philopatry, over prolonged time periods.

The mitochondrial dates reported here for Aboriginal Australian arrival and dispersal appear considerably older than recent estimates from nuclear-genomic data[12] that suggest a single ancestral population started to differentiate as recently as 10–32 ka, following an admixture event with Denisovans around 43 ka. The latter event, at least, is inconsistent with the Australian archaeological record that does not support the presence of Denisovans, indicating that any admixture must have occurred before the colonization of Sahul around 50 ka. This raises the possibility that the molecular-dating analyses of the nuclear-genomic data have been confounded by complex population histories, including multiple hominin introgressions[12] and/or patterns of selection (Supplementary Information). By contrast, when combined with detailed phylogeographical data, mitogenome dating may provide a less complex alternative to reconstructing human colonization patterns in situations such as Australia.

Online Content Methods, along with any additional Extended Data display items and Source Data, are available in the online version of the paper; references unique to these sections appear only in the online paper.

Received 9 August 2016; accepted 24 January 2017.
Published online 8 March 2017.

1. Roberts, R. G., Jones, R. & Smith, M. A. Thermoluminescence dating of a 50,000-year-old human occupation site in northern Australia. *Nature* **345,** 153–156 (1990).
2. O'Connell, J. F. & Allen, J. The process, biotic impact, and global implications of the human colonization of Sahul about 47,000 years ago. *J. Archaeol. Sci.* **56,** 73–84 (2015).

3. Lewis, S. E., Sloss, C. R., Murray-Wallace, C. V., Woodroffe, C. D. & Smithers, S. G. Post-glacial sea-level changes around the Australian margin: a review. *Quat. Sci. Rev.* **74,** 115–138 (2013).
4. Redd, A. J. & Stoneking, M. Peopling of Sahul: mtDNA variation in aboriginal Australian and Papua New Guinean populations. *Am. J. Hum. Genet.* **65,** 808–828 (1999).
5. Rasmussen, M. *et al.* An Aboriginal Australian genome reveals separate human dispersals into Asia. *Science* **334,** 94–98 (2011).
6. Fehren-Schmitz L. *et al.* A re-appraisal of the early Andean human remains from Lauricocha in Peru. *PloS One.* **10,** e0127141 (2015).
7. Bergström, A. *et al.* Deep roots for Aboriginal Australian Y chromosomes. *Curr. Biol.* **26,** 809–813 (2016).
8. Nagle, N. *et al.* Antiquity and diversity of aboriginal Australian Y-chromosomes. *Am. J. Phys. Anthropol.* **159,** 367–381 (2016).
9. Hudjashov, G. *et al.* Revealing the prehistoric settlement of Australia by Y chromosome and mtDNA analysis. *Proc. Natl Acad. Sci. USA* **104,** 8726–8730 (2007).
10. van Holst Pellekaan, S. Genetic evidence for the colonization of Australia. *Quat. Int.* **285,** 44–56 (2013).
11. Heupink, T. H. *et al.* Ancient mtDNA sequences from the First Australians revisited. *Proc. Natl Acad. Sci. USA* **113,** 6892–6897 (2016).
12. Malaspinas, A.-S. *et al.* A genomic history of Aboriginal Australia. *Nature* **538,** 207–214 (2016).
13. Reeves, J. M. *et al.* Palaeoenvironmental change in tropical Australasia over the last 30,000 years—a synthesis by the OZ-INTIMATE group. *Quat. Sci. Rev.* **74,** 97–114 (2013).
14. Fitzsimmons, K. E. *et al.* Late Quaternary palaeoenvironmental change in the Australian drylands. *Quat. Sci. Rev.* **74,** 78–96 (2013).
15. Williams, A. N., Ulm, S., Turney, C. S. M., Rohde, D. & White, G. Holocene demographic changes and the emergence of complex societies in prehistoric Australia. *PLoS One* **10,** e0128661 (2015).
16. Ulm, S. 'Complexity' and the Australian continental narrative: themes in the archaeology of Holocene Australia. *Quat. Int.* **285,** 182–192 (2013).
17. Sutton, P. *Native title in Australia: an ethnographic perspective.* (Cambridge Univ. Press, 2003).
18. Fu, Q. *et al.* A revised timescale for human evolution based on ancient mitochondrial genomes. *Curr. Biol.* **23,** 553–559 (2013).
19. Reimer, P. J. *et al.* IntCal13 and marine13 radiocarbon age calibration curves 0–50,000 years cal BP. *Radiocarbon* **55,** 1869–1887 (2013).
20. Bowdler, S. in *Sunda and Sahul: Prehistoric Studies in Southeast Asia, Melanesia and Australia* (eds Allen, J., Golson, J. & Jones, R.) 205–246 (Academic Press, 1977).
21. Bird, M. I., O'Grady, D. & Ulm, S. Humans, water, and the colonization of Australia. *Proc. Natl Acad. Sci. USA* **113,** 11477–11482 (2016).
22. Mcallister, P., Nagle, N. & Mitchell, R. J. Brief communication: the Australian Barrineans and their relationship to Southeast Asian negritos: an investigation using mitochondrial genomics. *Hum. Biol.* **85,** 485–502 (2013).
23. White, J. P. & O'Connell, J. F. *A Prehistory of Australia, New Guinea, and Sahul.* (Academic Press, 1982).
24. Hamm, G. *et al.* Cultural innovation and megafauna interaction in the early settlement of arid Australia. *Nature* **539,** 280–283 (2016).
25. Saltré, F. *et al.* Climate change not to blame for late Quaternary megafauna extinctions in Australia. *Nat. Commun.* **7,** 10511 (2016).
26. Roberts, R. G. *et al.* New ages for the last Australian megafauna: continent-wide extinction about 46,000 years ago. *Science* **292,** 1888–1892 (2001).
27. Metcalf, J. L. *et al.* Synergistic roles of climate warming and human occupation in Patagonian megafaunal extinctions during the last deglaciation. *Sci. Adv.* **2,** e1501682 (2016).
28. Williams, A. N., Ulm, S., Cook, A. R., Langley, M. C. & Collard, M. Human refugia in Australia during the Last Glacial Maximum and terminal Pleistocene: a geospatial analysis of the 25–12ka Australian archaeological record. *J. Archaeol. Sci.* **40,** 4612–4625 (2013).
29. Smith, M. *The Archaeology of Australia's Deserts* (Cambridge Univ. Press, 2013).
30. Llamas, B. *et al.* Ancient mitochondrial DNA provides high-resolution time scale of the peopling of the Americas. *Sci. Adv.* **2,** e1501385 (2016).
31. Drummond, A. J. & Rambaut, A. BEAST: Bayesian evolutionary analysis by sampling trees. *BMC Evol. Biol.* **7,** 214 (2007).
32. Posth, C. *et al.* Pleistocene mitochondrial genomes suggest a single major dispersal of non-Africans and a late glacial population turnover in Europe. *Curr. Biol.* **26,** 827–833 (2016).
33. Ho, S. Y. W. *et al.* Time-dependent rates of molecular evolution. *Mol. Ecol.* **20,** 3087–3101 (2011).
34. Rieux, A. & Balloux, F. Inferences from tip-calibrated phylogenies: a review and a practical guide. *Mol. Ecol.* **25,** 1911–1924 (2016).
35. Balme, J., Davidson, I., McDonald, J., Stern, N. & Veth, P. Symbolic behaviour and the peopling of the southern arc route to Australia. *Quat. Int.* **202,** 59–68 (2009).
36. Cooper, A. & Stringer, C. B. Paleontology. Did the Denisovans cross Wallace's Line? *Science* **342,** 321–323 (2013).

Supplementary Information is available in the online version of the paper.

Acknowledgements We acknowledge the support and involvement of the Point Pearce, Cherbourg and Koonibba communities and the individual families. We also acknowledge the work of N. Tindale, J. Birdsell and members of the original Board for Archaeological Research expeditions collecting the specimens. We thank the South Australian Museum, Australian Research Council, University of Adelaide Environment Institute, the Genographic Project and Bioplatforms Australia for support, and S. Ulm, G. Gower, I. Mathieson, L. O'Brien, S. Easteal, M. Vilar, C. Stringer and ACAD colleagues for helpful comments and advice. The Aboriginal Heritage Project webpage is https://www.adelaide.edu.au/acad/ahp/, and this work was carried out under the auspices of the University of Adelaide Human Research Ethics Committee, project approval H-2014-252.

Author Contributions The project was conceived by A.C., W.H. and P.S. and directed by A.C. and W.H. Archival research and community outreach was led by I.O., A.A-H., S.A., A.O., F.Z. and L.W. with A.C., W.H., R.T. and R.J.M. The genetic sequencing was performed and coordinated by W.H., P.B., M.W., S.R. and J.R.S., and the genetic analysis by W.H., R.T., A.R., J.S., J.T., N.B., B.L. and A.C. Archaeological and anthropological interpretations were provided by P.S., C.T., A.N.W. and K.W. The manuscript was written by A.C. and R.T., with critical input from P.S., C.T., A.N.W., A.R., J.S., W.H. and all other co-authors. R.T., J.S., A.N.W. and A.R. compiled the Supplementary Information.

Author Information Reprints and permissions information is available at www.nature.com/reprints. The authors declare no competing financial interests. Readers are welcome to comment on the online version of the paper. Correspondence and requests for materials should be addressed to A.C. (alan.cooper@adelaide.edu.au).

Reviewer Information *Nature* thanks P. Bellwood, C. Lalueza-Fox and the other anonymous reviewer(s) for their contribution to the peer review of this work.

METHODS

Samples. The 111 hair samples used in the present study were originally collected during anthropological expeditions to one of the following communities: Cherbourg, Queensland (23 samples), Point Pearce, South Australia (41 samples) and Koonibba, South Australia (47 samples) (Extended Data Fig. 1 and Supplementary Table 1). Consent was obtained from the original donors, or their descendants, according to protocols detailed in the Supplementary Information. Six of the Koonibba samples were collected during an expedition to the area between 13 and 25 August 1928, all remaining samples were obtained from the extensive Harvard and Adelaide Universities Anthropological Expeditions lead by N. B. Tindale and J. B. Birdsell that took place from 13 May 1938 to 30 June 1939. Hair was collected from different parts of the body, but all samples used in the current study consist of small locks of hair that were cut with permission from the head of participants. Since the initial collection date, the hair samples have been stored in sealed paper envelopes. The envelopes are currently secured in a restricted-access storage room maintained by the South Australian Museum. For each sample, a portion of the hair (between 20–190 mg) was removed from each envelope for use in the present study.

Ancient DNA analysis. The hair samples from Cherbourg and Point Pearce were soaked in 3.5 ml of 1% bleach, rinsed in 7 ml of water, and subsequently 3.5 ml of 100% ethanol and before being air-dried. For the Koonibba samples, we applied 2 washes in 3 ml of water, a subsequent wash in 3 ml of 100% ethanol, followed by air-drying. Each sample was digested for 1 h under constant rotation at 55 °C in 4 ml of a digestion buffer containing 75 mM Tris pH 8.0, 50 mM NaCl (Sigma-Aldrich), 0.5 mg ml^{-1} Proteinase K (Life Technologies), 50 mM DTT (Promega) and 0.75% SDS (Life Technologies). After lysis, samples were centrifuged at 4,600 r.p.m. for 1 min and the supernatant was pipetted into 100 µl silica suspension and 16 ml modified binding buffer (90% QG Buffer (Qiagen), 1.3% Triton X-100 (Sigma-Aldrich), 25 mM NaCl (Sigma-Aldrich) and 0.2 M sodium acetate (Sigma-Aldrich)), and left for 1 h at room temperature under constant rotation. Silica suspensions subsequently pelleted using a centrifuge at 4,600 r.p.m. for 5 min, and the supernatant was discarded. The silica pellet was washed three times in 80% ethanol and centrifugation at 13,000 r.p.m. for 1 min. After the last wash, the pellet was air dried for 30 min and resuspended twice in 120 µl of a pre-warmed (at 50 °C) mix of EB buffer (Qiagen) and 0.05% Tween 20, and incubated for 10 min. After centrifugation at 13,000 r.p.m. for 1 min, a final 240 µl extract was obtained. Subsequently, 60 µl extract was purified using a MinElute Reaction Cleanup Kit (Qiagen) following the manufacturer's protocol.

Double-stranded libraries were prepared following standard protocols[30,37,38], using short Illumina adapters with dual 5-mer (non-Koonibba samples) or 7-mer (Koonibba samples) internal barcodes. For the Koonibba samples partial uracil-DNA-glycosylase (UDG) treatment[39] was performed for DNA repair in the first step of library construction. Libraries for the Koonibba sample extracts were amplified using Platinum Taq HiFi (Invitrogen), whereas the Cherbourg and Point Pearce samples were amplified using isothermal amplification (TwistAmp Basic kit, TwistDx Ltd). The latter were enriched by hybridization using mitochondrial RNA baits prepared in-house and finally amplified using full-length 7-mer indexed Illumina adapters (see ref. 6 for a full explanation of the protocol). Libraries were pooled and sequenced in a HiSeq 2×100 PE run. The Koonibba libraries were amplified using full-length 7-mer indexed Illumina adapters and shotgun sequenced in MiSeq (2×150 PE) and NextSeq (2×150 PE) Mid Output runs at the Australian Genome Research Facility.

Mapping and consensus calling. Raw Illumina reads were processed using the PaleoMix v1.0.1[40] pipeline. AdapterRemoval v2 (ref. 41) was used to trim adaptor sequences, merge the paired reads, and eliminate all reads shorter than 25 bp. Filtered reads were then mapped to the Reconstructed Sapiens Reference Sequence (RSRS) mitochondrial reference genome[42] with BWA v0.6.2 (ref. 43). The minimum mapping quality was set to 25, seeding was disabled and the maximum number or fraction of open gaps was set to 2. MapDamage v2 (ref. 44) was used to check that the expected mapping and damage patterns were observed for each library and re-scale base qualities for the non-repaired libraries (see Supplementary Table 2 for library statistics).

All mtDNA genome consensus sequences were called using Geneious v9.1.3 (ref. 45). For each sample, reads were remapped to the RSRS reference using the Geneious mapper (default settings, serial mapping iterated five times). To call a base, each region required a coverage $\geq$3, with a majority allele frequency $\geq$0.75. The resulting consensus sequences were then inspected by eye, with particular attention being paid to the hypervariable regions and nucleotide positions previously identified as being problematic on the phylotree website (http://www.phylotree.org/)[46]. All ambiguous sites were called as 'N'.

Identical haplotypes were collapsed into a single haplotype sequence. Individuals with genealogical information that indicated a shared common maternal ancestor were checked for sequence similarity, and were identical in all but two cases where they differed by a single nucleotide. These cases were subsequently maintained as separate mtDNA haplotypes. For all individuals where identity by maternal descent was unknown, two sequences were deemed as identical if their sequences shared all diagnostic variants for a given haplogroup. After combining all common haplotypes, a total of 54 non-redundant consensus sequences were determined (from 111 original samples; Supplementary Table 1). The resulting consensus haplotypes cover all the major mtDNA haplogroups previously described for Australia (Supplementary Information).

Phylogenetics. To help determine the timing of the split between Melanesian and Australian populations, and the colonization history of Australia, the phylogenetic software BEAST (v1.8.3)[31,47] was used on 123 complete (or mostly complete) mtDNA genomes (54 unique Aboriginal Heritage Project (AHP) consensus samples combined with 44 Australian and 25 Melanesian publicly available sequences; see Supplementary Table 1). The non-AHP sequences were obtained from the mitochondrial database mtDB[48] and two recently published papers[5,11]. Before analysis, all 123 mtDNA genomes were aligned to the RSRS with BLAT[49] and then analysed with a custom R script, so that indels were removed and only point mutations relative to the RSRS were used in the subsequent analyses.

The TN93+G6 model of nucleotide substitution was selected through comparison of BIC scores using ModelGenerator v0.85 (ref. 50), a GMRF skyride model[51] was used to allow for a complex population history, with a relaxed uncorrelated log-normal clock[52] to account for rate heterogeneity between lineages (a strict clock was empirically rejected as ucld.stdev posterior distribution did not include zero). Monophyly was constrained for all major haplogroups and the ancient sequence hap97 was given a tip date log-normal prior distribution with a mean of 1,250 years and a standard deviation of 0.7 (95% of the dates fall between 500 and 3,000 years; based on estimates from ref. 11). Two mutation rates with normally distributed priors were applied, using the values from ref. 18 (mean = 2.67×10^{-8} substitutions per site per year, s.d. = 2.6×10^{-9}) and from ref. 32 (mean = 2.74×10^{-8} substitutions per site per year, s.d. = 2×10^{-9}). These two rate estimates were chosen as they both use state of the art tip-dating calibration methods to infer mutation rates, thereby providing inferences that minimise the effects of rate temporal dependency on late Palaeolithic events[33,34]. In particular, the mutation-rate estimates reported in refs 18,32 are based on 10 and 66 radiocarbon-dated ancient sequences, respectively. Notably, the calibration dates for these ancient sequences are distributed across 46,000–4,000 ka and cover both haplogroups M and N, a scenario that is well–suited for comparison with Australia, both in terms of temporal coverage and mtDNA diversity. Separate BEAST phylogenies were inferred for the combined set of Melanesian and Australian lineages using the mutation rate from ref. 18 (Fig. 1 and Extended Data Fig. 2) and ref. 32 (Extended Data Fig. 3). A phylogeny based on Australian lineages only was also inferred using the mutation rate from ref. 18 and used to determine the palaeodemography of Australia (Extended Data Fig. 7).

All parameters showed sufficient sampling (indicated by effective sample sizes above 200) after 20,000,000 steps, with the first 10% of samples discarded as burn-in. Notably, the two different mutations rates produced TMRCA estimates for the major haplogroups within 1.5 kyr of each other (Extended Data Figs 2, 3), with posterior mutation-rate estimates that were also highly similar (mean rate = 2.70×10^{-8} (ref. 18), mean rate = 2.74×10^{-8} (ref. 32)), indicating that the choice of prior distribution for the mutation rate had little effect on our dating.

Multiple correspondence analyses. A useful tool for detecting and analysing demographic structure in genetic data is principal components analysis (PCA)[53]. When working with non-autosomal data, PCA cannot be applied to any (satisfactory) recoding of sequence data (unless it is manually, that is, subjectively, sorted into haplogroups). Multiple correspondence analysis (MCA) is an analysis technique for data exploration and dimension reduction for categorical data. MCA is a generalization of PCA to categorical variables and can therefore be applied to raw sequence data. MCA has been independently rediscovered many times since its original development, and as such can also be found under titles including 'optimal scaling', 'dual scaling' and 'homogeneity analysis'[54]. MCA was originally developed for the analysis of survey data, so that responses that were commonly (or rarely) reported together could be efficiently identified. We apply the same notion but treat single nucleotide polymorphisms (SNPs) as survey questions, and observed SNP markers as responses.

We restricted the MCA to AHP samples and two Australian mtDNA haplotypes derived from ancient samples whose origin was assumed to be the area in which the specimen was collected[5,11] (Supplementary Table 3). Unfortunately, we have been unable to obtain the mtDNA data from a recent Aboriginal genomics study[12] to use in the MCA analyses, although these samples may have had limited utility for phylogeographic analysis given the large-scale relocation of Aboriginal Australians after European arrival. However, we have included the reported sample locations and mtDNA lineages in geographic plots to examine the consistency with our results (Extended Data Fig. 4). For the AHP samples, geographic locations were

determined for each individual using the relevant genealogies to trace maternal ancestry as far back as the archival information allowed. Importantly, the broad distribution of the female ancestors for the AHP samples collected from each of the three sampling locations (Extended Data Fig. 1) reflects the forced relocation of Aboriginal Australians from their traditional territories, and highlights the difficulties associated with obtaining valid phylogeographic information using only modern samples.

Identical samples were treated separately if they came from different geographical locations, as these most likely represented more distant family relationships not captured in the genealogical information. This resulted in 76 unique sequences (Supplementary Table 3). Restricting the analyses to these samples ensured that the underlying phylogeographic signal was not diluted by the addition of sequences from modern individuals that are likely to have been affected by forced-displacement or child-removal policies and typically lack genealogical information. Independent MCA analyses were run for all samples combined and for each haplogroup separately. We excluded the M16 lineage from the M haplogroup tests, because this was a deeply divergent Australian lineage that clusters among Melanesian samples and thereby most likely represents a pre-Sahul split (Fig. 1).

We cleaned the aligned sequence data by removing any homogeneous (uninformative) sites, and any sites containing missing data. Unlike PCA analyses, we are not forced to filter out triallelic SNPs and thereby can retain the information contained within these sites[53]. For M sequences in an alignment, the MCA analysis will return $M-1$ principal dimensions of length $J-Q$, where Q is the number of cleaned SNPs of interest, and J is given by,

$$J = \sum_{i=1}^{Q} J_i$$

where J_i is the number of alleles observed at SNP i, for $i = 1, \ldots, Q$. These principal dimensions are analogous to the principal components returned from PCA analyses, and the dimensions are ordered by the amount of inertia (analogous to variability in PCA) that they explain. Dimensions with associated eigenvalues less than $1/Q$ are discarded as they explain less variation than expected (analogous to the threshold of 1 for the eigenvalues in PCA)[55]. The retained coordinates are then used for the visualization of the relationships between individuals, investigation of correlation between the dimensions and geographic variables, and clustering for genetic similarity. We carried out our MCA analysis using the FactoMineR package[56].

Clustering via *k* medoids. Identifying points in n-dimensional space based on similarity inferred through Euclidean distance is not a new problem. By far the most popular clustering algorithm is the k-means clustering algorithm[57]. We used the closely related k-medoids algorithm instead, which, instead of using a centroid for each cluster, forces one of the observed data points to be the centre of the cluster. In doing so, the inter- and intra-cluster distances are more robust to noise and outliers[58]. We consider an exhaustive range of values for k, and a 'best' number of clusters must be chosen. Unlike the possibly subjective 'elbow method', used in PCA through scree plots, we instead calculate $\bar{s}_k$, called the 'average silhouette'[59], for each value of k. The value of k that maximises $\bar{s}_k$ is chosen. However to avoid 'over-fitting' the number of clusters, we apply a leave-one-out jack-knife approach to both identify if influential individuals exist in the data and to obtain some measure of variability for the values of $\bar{s}_k$. We carried out our clustering methodology using the cluster package[60], in the R statistical programming language[61].

Testing for correlation. We tested for geographic correlation through two methods that seem similar, but are subtly different in their interpretation. First we applied the Mantel test, which is a test for correlation between two distance matrices[62]. One distance matrix contains the pairwise Euclidean distances between individuals with respect to their geographic location, and the second distance matrix contains the genetic distances, calculated from the coordinates of the MCA. The null hypothesis is that there is a perfectly mixed population (that is, pan-mixia), so that rejection of the null hypothesis indicates some genetic clustering on the landscape. At the cost of statistical power, we use the Spearman correlation coefficient, as it is unreasonable to assume strictly linear relationships. We used 10^5 permutations for each test. Second, we calculated the correlation between the longitude and latitude of individuals, and the retained principal dimensions. We perform a standard test for correlation under Spearman's ρ (for the same reasons indicated in the Mantel test). All tests of correlation use the AS 89 algorithm for calculation of P values[63].

Although these tests may appear similar, the Mantel test is a relative test of geographic correlation that simply tests for some clustering with respect to local geographic location. In essence, the Mantel test investigates if certain combinations of SNP markers are often found within close proximity. With the test of significant correlations between the principal dimensions and either longitude or latitude, not only distance, but also direction is important. Hence, the correlation tests are absolute tests for identifying if combinations of certain SNP markers can be linked to certain geographical locations on the landscape, with respect to the entire sampling region. We performed the Mantel test using the vegan package[64], and the standard correlation tests in the R statistical programming language[61]. The full list of P values from Spearman's correlation and the Mantel tests are shown in Extended Data Table 1.

The Australian archaeological record. *Devil's Lair, southwest Australia.* To more precisely constrain the time of arrival of modern humans in southwest Australia, we analysed a comprehensive multi-dating suite of ages for Devil's Lair, one of the earliest archaeological sites in southwestern Australia[65]. The dates comprise radiocarbon dating (pretreated using acid–base–acid or ABA, and acid–base–acid stepped combustion, or ABOX–SC, pretreatment), optically stimulated luminescence, electron-spin resonance (derived using an early uptake model) and U-series dating. Devil's Lair (34° 9′ S, 115° 4′ E) is a single-chamber cave (floor area 200 m^2) formed in the Quaternary dune limestone of the Leeuwin–Naturaliste Ridge, 5 km from the modern coastline and approximately 250 km south of Perth (Western Australia). Archaeological investigation over the past four decades has identified a stratigraphic sequence in the cave floor deposit that consists of 660 cm of sandy sediments, with >100 distinct layers, intercalated with flowstone and other indurated deposits[65–67]. Archaeological evidence for intermittent human occupation extends down to layer 30 (around 350 cm depth), with hearths, bone and stone artefacts found throughout. The lower part of layer 30 represents a fan of redeposited topsoil that accumulated rapidly after widening of the cave mouth, and contains the earliest evidence for occupation of the cave. Below layer 30, six stone artefacts have been identified, including a single specimen each from layers 32–35, 37 and 38. No artefacts have been found below layer 38.

The age model was created with OxCal v.4.2.4 using a Poisson process deposition model (P_sequence)[68] with the 'general outlier' analysis option[69] of all ages as reported in ref. 65. The outlier option was used to detect ages that fall outside the calibration model for the sequence and, if necessary, down-weight their contribution to the final age estimates. Radiocarbon ages were calibrated using the SHCal13 calibration dataset[70]. Taking into account the deposition model and the actual age measurements, the posterior probability densities quantify the most probable age distributions. Notably, the lowest artefact in the sequence is constrained by age estimates obtained using all four dating techniques (but excluding the ABA radiocarbon (^{14}C) ages, which reached background levels around 40 ka)[65], providing confidence in the calculated age for this level. Using this approach we derive an age for layer 30 (lower) for cave occupation of 47.1 ± 0.8 ka and the lowest artefact (layer 38) of 49.5 ± 1.1 ka (Extended Data Fig. 5).

Early colonization of Australia. We extended this approach across Australia, and examined radiocarbon and optically stimulated luminescence ages associated with the lowest cultural horizons in early Australian archaeological sites (Extended Data Fig. 6 and Supplementary Table 4) to estimate the timing of colonization across the continent. Here we used the Phase model option in OxCal v.4.2.4 (ref. 68) with general outlier analysis detection (probability = 0.05)[69]. Notably, the Phase option is a grouping model which assumes no geographic relationship between samples (in contrast to the P_sequence used above, which assumes a stratigraphic relationship between dated levels). The model simply assumes that the ages represent a uniform distribution between a start and end boundary[68]. Terrestrial samples were calibrated using the SHCal13 dataset[70]; marine ages were converted to calendar ages using the Marine13 calibration dataset[19] and corrected for regional ΔR (marine reservoir age) with reported values for Papua New Guinea (372 ± 64 years)[71] and the east Indian Ocean (43 ± 81 years)[72,73]. Using this approach, and incorporating the age calculated above from Devil's Lair, we derive an age estimate for human arrival in Australia (the start of continental occupation) as 48.8 ± 1.3 ka (Extended Data Fig. 3). Notably, this age estimate includes the luminescence-dated Northern Territory sites of Malakunanja II and Nauwalabila I (ref. 74–76), which are statistically indistinguishable from the timing of occupation continent-wide. Our estimated timing of human arrival is consistent with the minimum age obtained from the Huon Peninsula[77,78] and the recently reported ages obtained from Warratyi Rockshelter in the Flinders Ranges[24].

Data availability. The datasets generated and analysed during the current study are available in the European Nucleotide Archive repository, and are accessible through accession number PRJEB15344. Additional data related to this paper may be requested from the authors.

37. Meyer, M. & Kircher, M. Illumina sequencing library preparation for highly multiplexed target capture and sequencing. *Cold Spring Harb. Protoc.* **2010,** pdb.prot5448 (2010).
38. Knapp, M., Stiller, M. & Meyer, M. Generating barcoded libraries for multiplex high-throughput sequencing. *Methods Mol. Biol.* **840,** 155–170 (2012).
39. Rohland, N., Harney, E., Mallick, S., Nordenfelt, S. & Reich, D. Partial uracil-DNA-glycosylase treatment for screening of ancient DNA. *Phil. Trans. R. Soc. Lond. B* **370,** 20130624 (2015).

40. Schubert, M. *et al.* Characterization of ancient and modern genomes by SNP detection and phylogenomic and metagenomic analysis using PALEOMIX. *Nat. Protocols* **9,** 1056–1082 (2014).
41. Lindgreen, S. AdapterRemoval: easy cleaning of next-generation sequencing reads. *BMC Res. Notes* **5,** 337 (2012).
42. Behar, D. M. *et al.* A "Copernican" reassessment of the human mitochondrial DNA tree from its root. *Am. J. Hum. Genet.* **90,** 675–684 (2012).
43. Li, H. & Durbin, R. Fast and accurate short read alignment with Burrows–Wheeler transform. *Bioinformatics* **25,** 1754–1760 (2009).
44. Jónsson, H., Ginolhac, A., Schubert, M., Johnson, P. L. F. & Orlando, L. mapDamage2.0: fast approximate Bayesian estimates of ancient DNA damage parameters. *Bioinformatics* **29,** 1682–1684 (2013).
45. Kearse, M. *et al.* Geneious basic: an integrated and extendable desktop software platform for the organization and analysis of sequence data. *Bioinformatics* **28,** 1647–1649 (2012).
46. van Oven, M. & Kayser, M. Updated comprehensive phylogenetic tree of global human mitochondrial DNA variation. *Hum. Mutat.* **30,** E386–E394 (2009).
47. Drummond, A. J., Suchard, M. A., Xie, D. & Rambaut, A. Bayesian phylogenetics with BEAUti and the BEAST 1.7. *Mol. Biol. Evol.* **29,** 1969–1973 (2012).
48. Ingman, M. & Gyllensten, U. mtDB: Human mitochondrial genome database, a resource for population genetics and medical sciences. *Nucleic Acids Res.* **34,** D749–D751 (2006).
49. Kent, W. J. BLAT—the BLAST-like alignment tool. *Genome Res.* **12,** 656–664 (2002).
50. Keane, T. M., Creevey, C. J., Pentony, M. M., Naughton, T. J. & Mclnerney, J. O. Assessment of methods for amino acid matrix selection and their use on empirical data shows that ad hoc assumptions for choice of matrix are not justified. *BMC Evol. Biol.* **6,** 29 (2006).
51. Minin, V. N., Bloomquist, E. W. & Suchard, M. A. Smooth skyride through a rough skyline: Bayesian coalescent-based inference of population dynamics. *Mol. Biol. Evol.* **25,** 1459–1471 (2008).
52. Drummond, A. J., Ho, S. Y. W., Phillips, M. J. & Rambaut, A. Relaxed phylogenetics and dating with confidence. *PLoS Biol.* **4,** e88 (2006).
53. Patterson, N., Price, A. L. & Reich, D. Population structure and eigenanalysis. *PLoS Genet.* **2,** e190 (2006).
54. Abdi, H. & Valentin, D. in *Encyclopedia of Measurement and Statistics* (ed. Salkind, N.) 651–657 (Thousand Oaks, 2007).
55. Greenacre, M. *Correspondence Analysis in Practice.* (CRC Press, 2007).
56. Lê, S., Josse, J. & Husson, F. FactoMineR : an R package for multivariate analysis. *J. Stat. Softw.* **25,** 1–18 (2008).
57. Lloyd, S. P. Least squares quantization in PCM. *IEEE Trans. Inf. Theory* **28,** 129–137 (1982).
58. Kaufman, L. & Rousseeuw, P. J. Clustering by means of medoids. *Statistical Data Analysis Based on the L 1-Norm and Related Methods. First International Conference* 405–416416 (1987).
59. Rousseeuw, P. J. Silhouettes: a graphical aid to the interpretation and validation of cluster analysis. *J. Comput. Appl. Math.* **20,** 53–65 (1987).
60. Maechler, M., Rousseeuw, P., Struyf, A., Hubert, M. & Hornik, K. Cluster Analysis Basics and Extensions. R package version 2.0.4. *CRAN* (2016).
61. R Development Core Team. R: a language and environment for statistical computing. *R Foundation for Statistical Computing, Vienna, Austria* http://www.R-project.org (2013).
62. Legendre, P. & Fortin, M. J. Comparison of the Mantel test and alternative approaches for detecting complex multivariate relationships in the spatial analysis of genetic data. *Mol. Ecol. Resour.* **10,** 831–844 (2010).
63. Best, D. J. & Roberts, D. E. Algorithm AS 89: The upper tail probabilities of Spearman's *Rho. Appl. Stat.* **24,** 377–379 (1975).
64. Dixon, P. VEGAN, a package of R functions for community ecology. *J. Veg. Sci.* **14,** 927–930 (2003).
65. Turney, C. S. M. *et al.* Early human occupation at Devil's Lair, southwestern Australia 50,000 years ago. *Quat. Res.* **55,** 3–13 (2001).
66. Dortch, C. E. & Dortch, J. Review of Devil's Lair artefact classification and radiocarbon chronology. *Aust. Archaeol.* **43,** 28–32 (1996).
67. Dortch, C. Devil's Lair, an example of prolonged cave use in South-Western Australia. *World Archaeol.* **10,** 258–279 (1979).
68. Bronk Ramsey, C. & Lee, S. Recent and planned developments of the program OxCal. *Radiocarbon* **55,** 720–730 (2013).
69. Bronk Ramsey, C. Dealing with outliers and offsets in radiocarbon dating. *Radiocarbon* **57,** 1023–1045 (2009).
70. Hogg, A. *et al.* SHCal13 Southern Hemisphere calibration, 0–50,000 years cal BP. *Radiocarbon* **55,** 1889–1903 (2013).
71. Petchey, F., Phelan, M. & White, J. P. New ΔR values for the southwest Pacific Ocean. *Radiocarbon* **46,** 1005–1014 (2004).
72. O'Connor, S., Ulm, S., Fallon, S. J., Barham, A. & Loch, I. Pre-bomb marine reservoir variability in the Kimberley region, Western Australia. *Radiocarbon* **52,** 1158–1165 (2010).
73. Bowman, G. M. Oceanic reservoir correction for marine radiocarbon dates from northwestern Australia. *Aust. Archaeol.* **20,** 58–67 (1985).
74. Roberts, R. G. *et al.* The human colonisation of Australia: optical dates of 53,000 and 60,000 years bracket human arrival at Deaf Adder Gorge, Northern Territory. *Quat. Sci. Rev.* **13,** 575–583 (1994).
75. Roberts, R. G. *et al.* Single-aliquot and single-grain optical dating confirm thermoluminescence age estimates at Malakunanja II rock shelter in northern Australia. *Anc. TL* **16,** 19–24 (1998).
76. Bird, M. I. *et al.* Radiocarbon dating of organic- and carbonate-carbon in *Genyornis* and *Dromaius* eggshell using stepped combustion and stepped acidification. *Quat. Sci. Rev.* **22,** 1805–1812 (2003).
77. Groube, L., Chappell, J., Muke, J. & Price, D. A 40,000 year-old human occupation site at Huon Peninsula, Papua New Guinea. *Nature* **324,** 453–455 (1986).
78. Roberts, R. G. Luminescence dating in archaeology: from origins to optical. *Radiat. Meas.* **27,** 819–892 (1997).

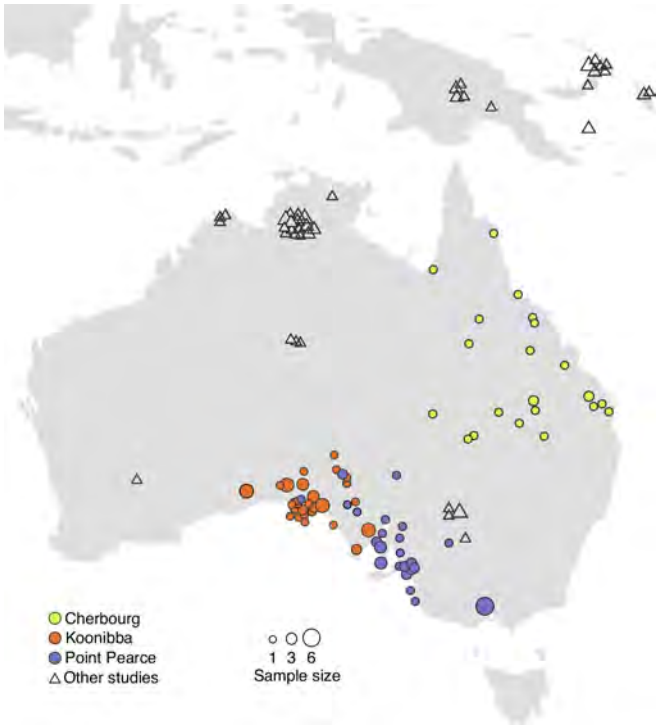

Extended Data Figure 1 | The geographical distribution of the oldest recorded maternal ancestors for the hair sample donors. Despite being collected from three different historical locations—Cherbourg (Queensland), Point Pearce and Koonibba (both South Australia)—the broad distribution of the maternal ancestors of the hair sample donors demonstrates the massive displacement experienced by Aboriginal Australians after European colonization. This pattern illustrates why the accurate reconstruction of Aboriginal Australian genetic history ultimately relies upon samples or genealogical records that capture patterns prior to this displacement. Map data was sourced from the Oak Ridge National Laboratory Distributed Active Archive Center (https://webmap.ornl.gov/wcsdown/wcsdown.jsp?dg_id=10003_1).

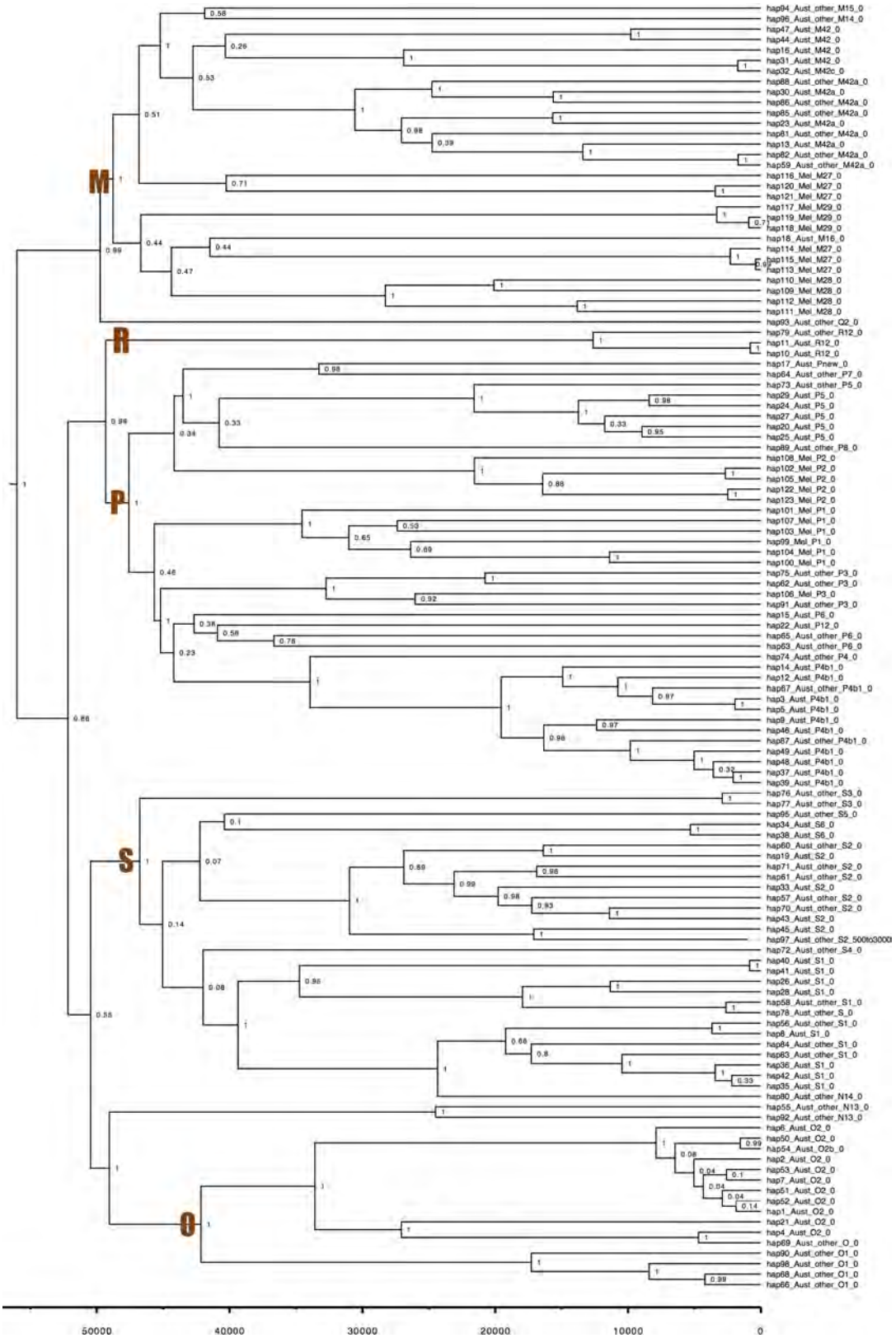

Extended Data Figure 2 | Sahul phylogenetic tree calibrated using the mitogenome rate from ref. 18. BEAST[31] phylogenetic tree of 123 Australian and Melanesian mtDNA lineages, which was calibrated using the ancient mitogenome rate in ref. 18 to minimize the impacts of temporal dependency[33,34] and improve estimation of the timing of the founding migrations. The major mitogenome haplogroups are shown at the base of each clade, and posterior support values are provided for all nodes.

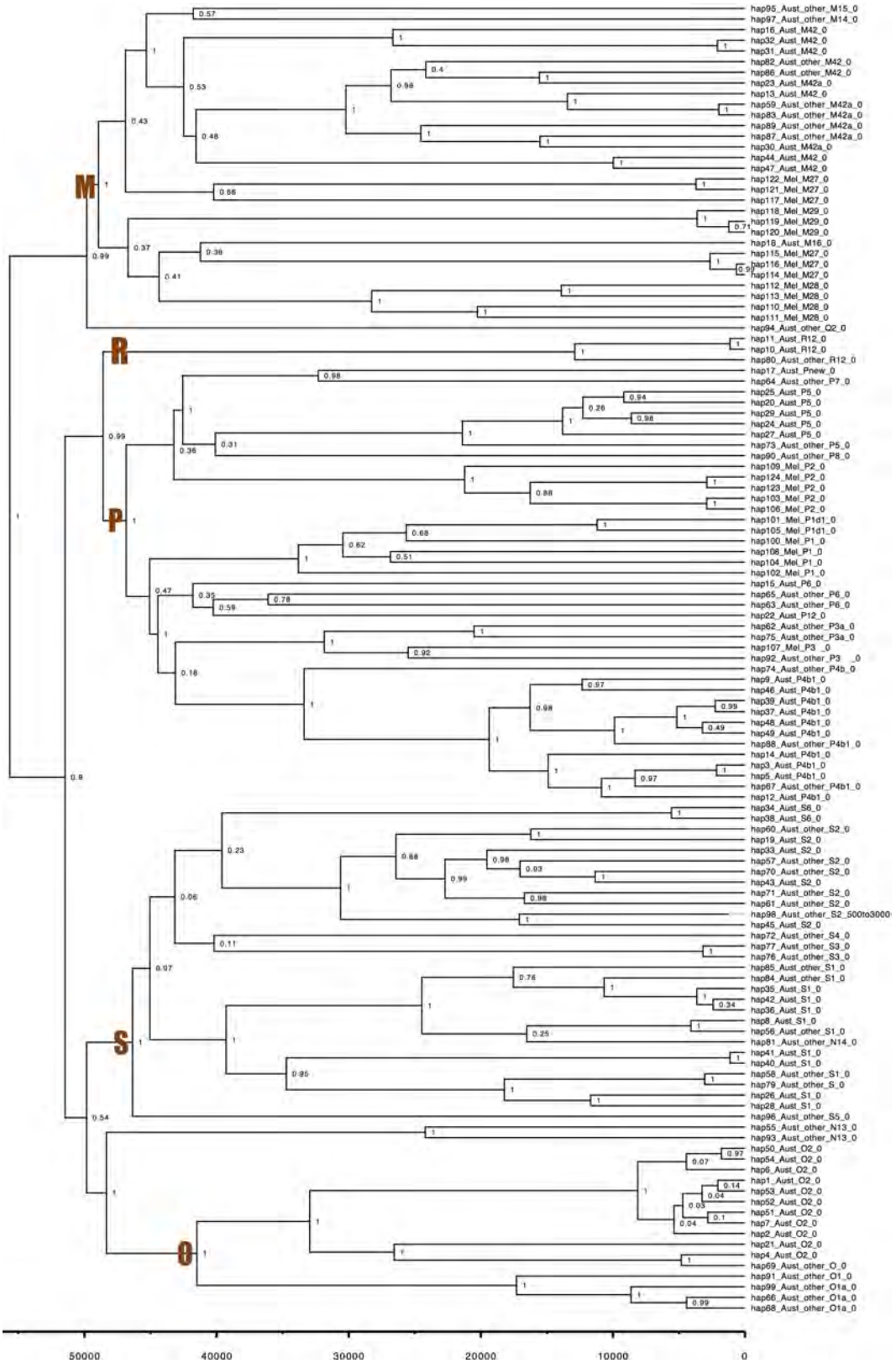

Extended Data Figure 3 | Sahul phylogenetic tree calibrated using mitogenome rate from ref. 32. As for Extended Data Fig. 2, except that rate calibration used the mitogenome rate from ref. 32.

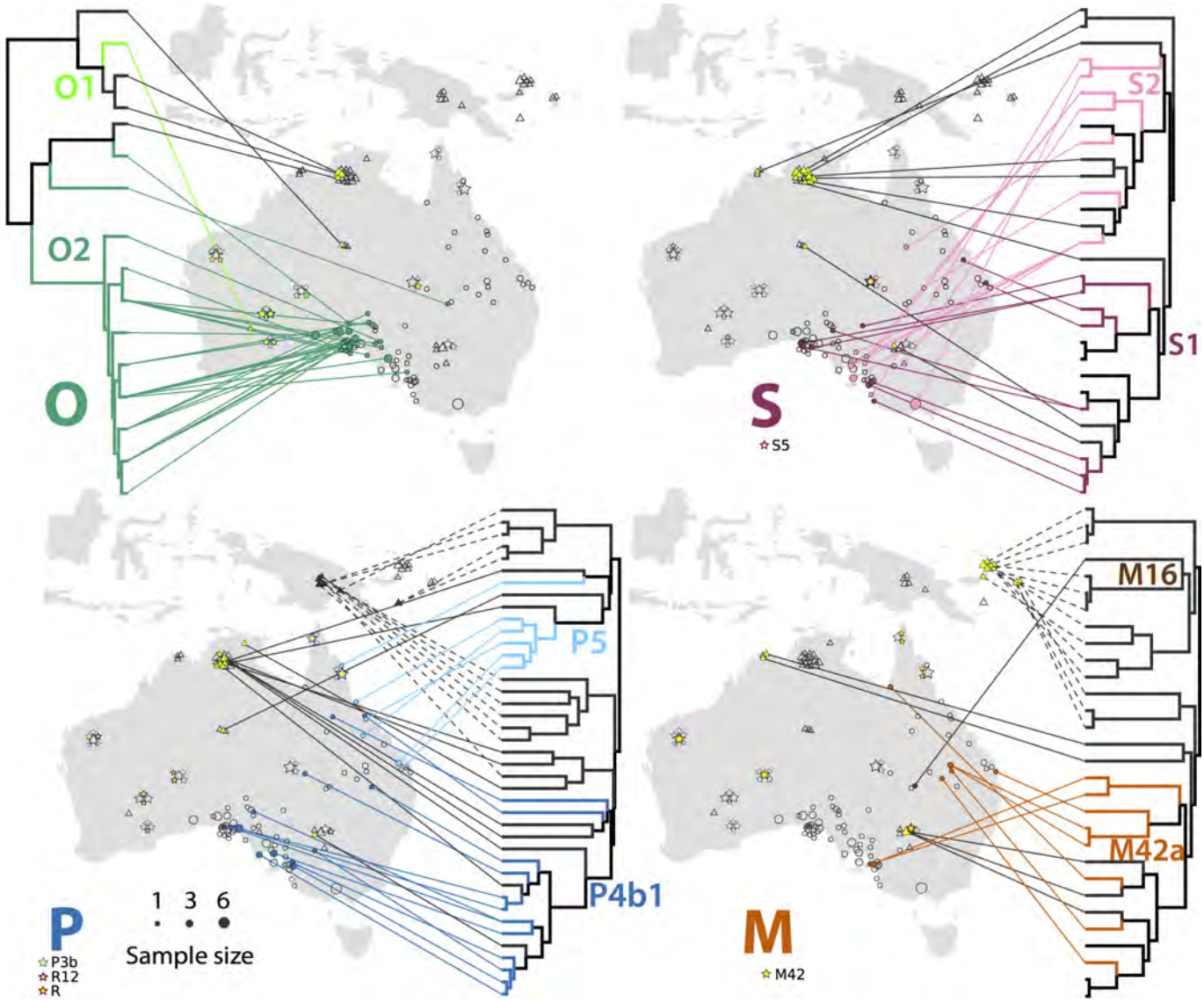

Extended Data Figure 4 | Australian phylogeography incorporating mtDNA lineage information from modern samples reported in ref. 12. The additional samples from ref. 12 are shown as stars and are distributed according to their reported locations of collection, all other sample information is presented in an identical manner to Fig. 2. The mtDNA haplogroups from ref. 12 are coloured according to the system used in Fig. 2, with haplogroups not previously shown (that is, R, R12, M42, P3b and S5) indicated with new colours that are described beneath the relevant haplogroup map (we have added the two R haplogroups on the P haplogroup map, as this is the closest sister clade). As in Fig. 2, mtDNA samples from other studies are shown in yellow, with the samples from ref. 12 having a yellow dot to indicate this status. Map data was sourced from the Oak Ridge National Laboratory Distributed Active Archive Center (https://webmap.ornl.gov/wcsdown/wcsdown.jsp?dg_id=10003_1).

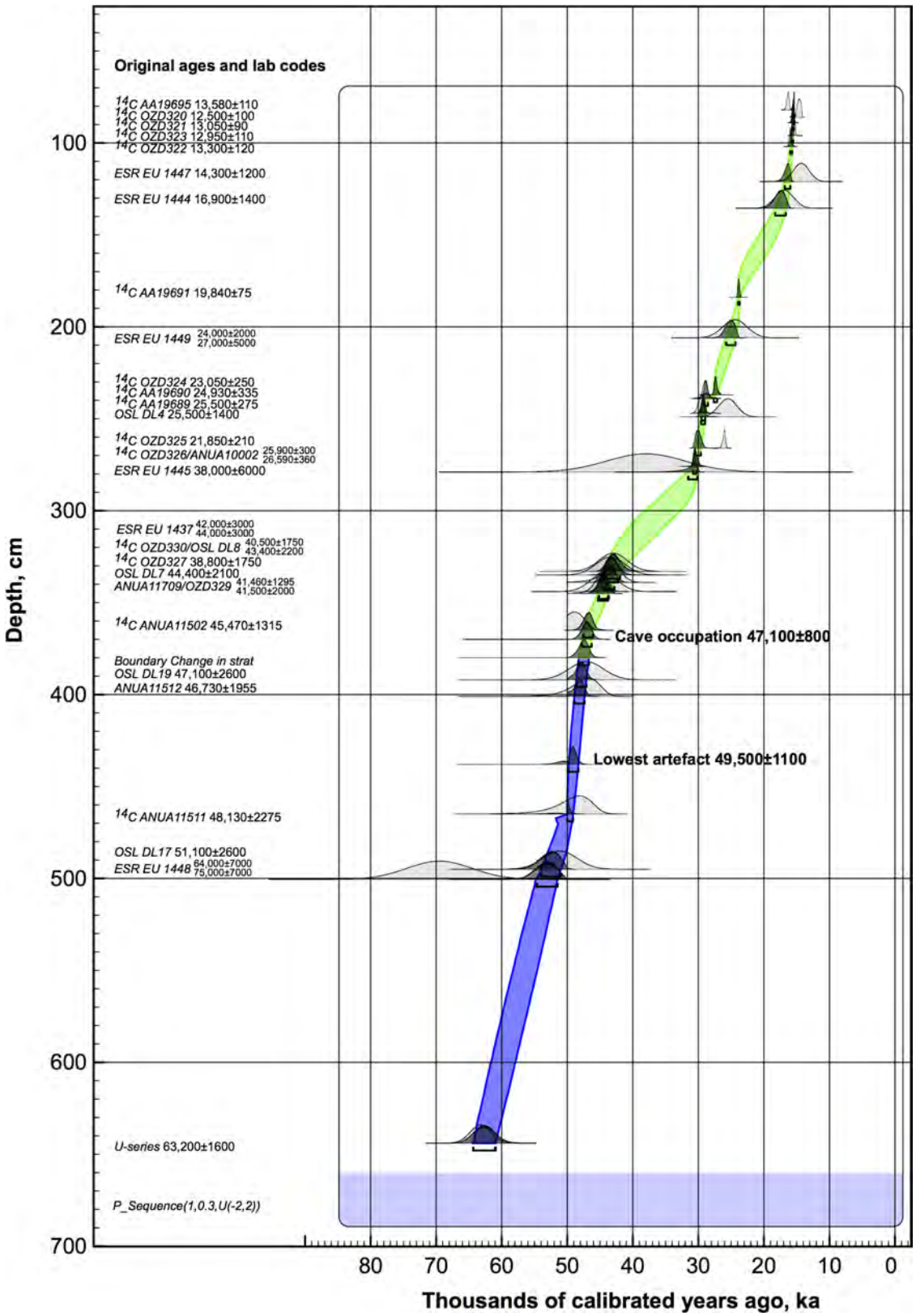

Extended Data Figure 5 | Age-depth model for Devil's Lair, south-western Australia. The age-depth model was generated with OxCal v.4.2.4 (ref. 68) using the Poisson process (outlier) deposition model. Original ages with 68% uncertainty (prior to modeling) with laboratory codes shown on left hand side. Prior (light grey) and posterior (dark grey) probability distributions are plotted. The blue and green envelopes describe the 68% confidence interval for the sedimentary units below and above layer 30 (lower) respectively.

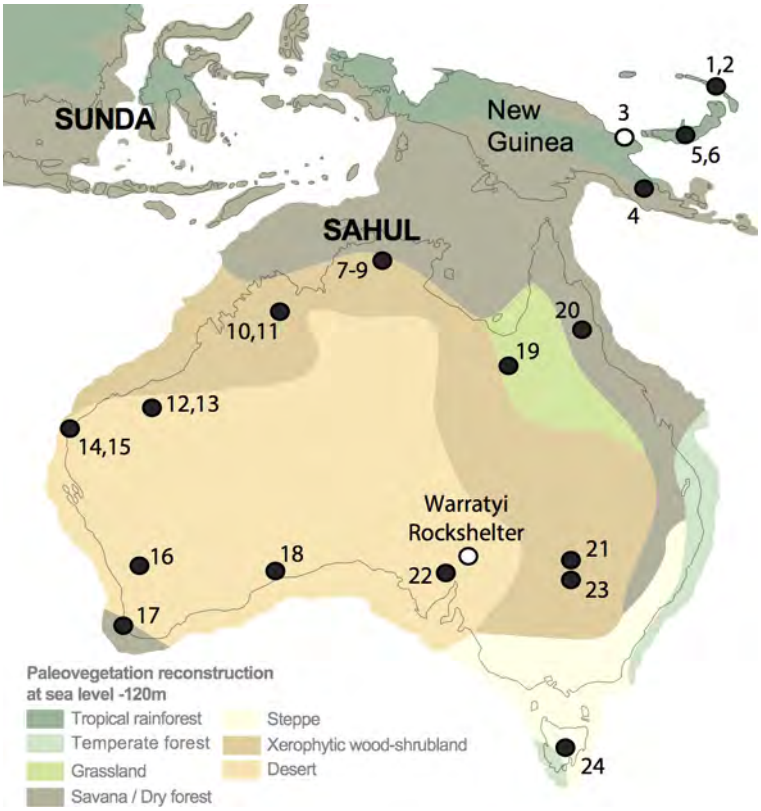

Extended Data Figure 6 | Locations of the early occupation sites used to estimate the timing of the colonization of Sahul. Sites used for colonization time estimation are shown as black dots, with white dots indicating sites that were used to provide independent age controls. Sites names: 1, Buang Merabak; 2, Matenkupkum; 3, Huon Peninsula; 4, Ivane; 5, Kupona na Dari; 6, Yombon; 7, Nawarla Gabarnmang; 8, Malakunanja II; 9, Nauwalabila I; 10, Carpenter's Gap; 11, Riwi; 12, Djadjiling; 13, Ganga Mara; 14, Jansz; 15, Mandu Mandu; 16, Upper Swan; 17, Devil's Lair; 18, Allen's Cave; 19, GRE8; 20, Ngarrabullgan; 21, Menindee; 22, Cooper's Dune (PACD H1); 23, Lake Mungo; and 24, Warreen Cave. Additional information for these sites including phase calibrated age ranges for initial occupation is provided in Supplementary Table 4. Phase calibrations were performed using OxCal v.4.2.4 (ref. 68) and resulted in an estimate of the initial colonization of Sahul at 48.8 ± 1.3 ka. The map was adapted from the figure in ref. 36, originally constructed by J.S.

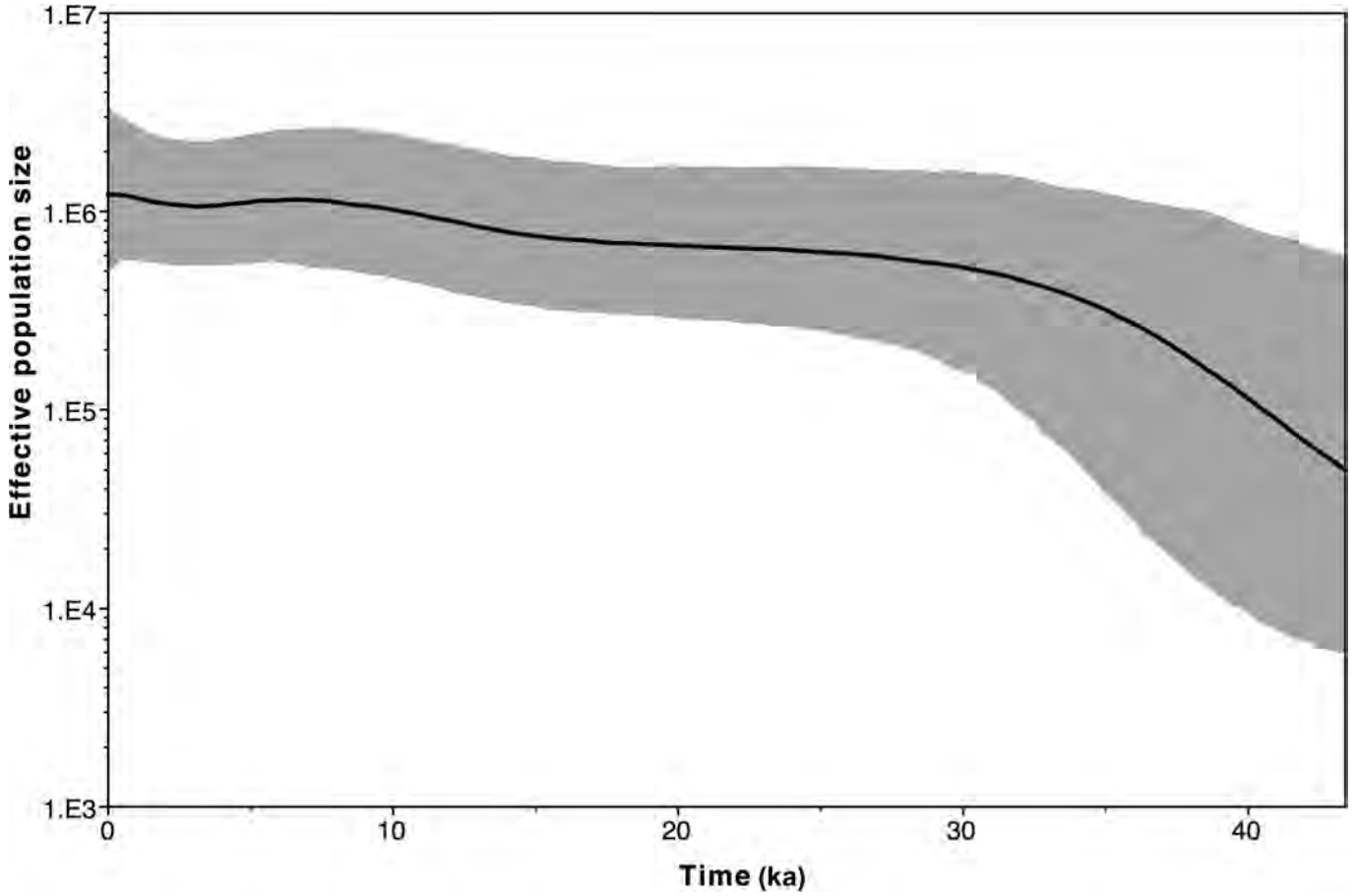

Extended Data Figure 7 | Palaeodemography of Australian mitogenomes. GMRF Skyride[51] analysis of the 98 Australian-only mtDNA lineages showing the estimated effective maternal population size since the initial colonization of Sahul around 50 ka (see Methods). Owing to the lack of available calibration points, the palaeodemographic curve should be considered relatively approximate. Nonetheless, there is no obvious indication of a major population bottleneck during the Last Glacial Maximum (around 21–18 ka). Line, median and grey shading, 95% highest posterior densities.

Extended Data Table 1 | Complete Australian phylogeography test results

Haplogroup	Metric	Dimension 1	Dimension 2	Dimension 3	Dimension 4	Dimension 5
M	Longitude	-0.3194 (0.3474)	0.642 (0.0929)*	-0.32 (0.2476)	0.6072 (0.1615)	NA
	Latitude	0.2310 (0.5444)	0.8560 (0.0055)***	0.4444 (0.4118)	0.0970 (0.6314)	NA
	CI%	42.30	70.30	84.76	93.96	NA
	Mantel Test			0.3273 (0.0953)*		
O	Longitude	0.0429 (0.9258)	-0.6395 (0.0629)*	0.5677 (0.3067)	NA	NA
	Latitude	0.5010 (0.0083)***	0.0002 (0.3935)	0.2923 (0.2174)	NA	NA
	CI%	47.86	75.10	98.18	NA	NA
	Mantel Test			0.3352 (0.0176)***		
P	Longitude	0.7796 (0.0002)***	-0.0703 (0.0053)***	-0.2378 (0.0048)***	-0.0360 (0.0169)**	NA
	Latitude	0.8690 (4e-6)***	0.0260 (0.9190)	-0.0101 (0.1155)	0.2300 (0.9811)	NA
	CI%	38.02	63.18	82.91	90.45	NA
	Mantel Test			0.4488 (3e-6)***		
P4b1	Longitude	-0.1940 (0.2557)	-0.1639 (0.1457)	NA	NA	NA
	Latitude	0.4826 (0.0035)***	0.2675 (0.0587)*	NA	NA	NA
	CI%	42.97	74.44	NA	NA	NA
	Mantel Test			-0.08687 (0.6008)		
P5	Longitude	0.08780 (0.0417)**	0.0556 (0.6083)	NA	NA	NA
	Latitude	-0.7540 (0.1167)	-0.2400 (0.3417)	NA	NA	NA
	CI%	41.49	67.07	NA	NA	NA
	Mantel Test			0.1152 (0.3750)		
S	Longitude	-0.1578 (0.5242)	0.1689 (0.1097)	0.3301 (0.1597)	0.6798 (0.0404)**	0.3351 (0.0016)***
	Latitude	-0.0797 (0.6019)	-0.2512 (0.8633)	0.5977 (0.0006)***	0.2175 (0.8720)	0.1020 (0.1780)
	CI%	26.87	50.25	68.84	81.60	89.56
	Mantel Test			0.2695 (0.0374)**		
All	Longitude	0.3807 (0.0003)***	0.2482 (0.0137)**	NA	NA	NA
	Latitude	0.1748 (0.0617)*	0.1059 (0.1765)	NA	NA	NA
	CI%	12.87	21.43	NA	NA	NA
	Mantel Test			0.2827 (7e-5)***		

Spearman's ρ for correlation with longitude, latitude (with associated P value in parentheses; *$P < 0.1$; **$P < 0.05$; ***$P < 0.01$) and the cumulative percentage of inertia (CI%, confidence interval) captured for each principal dimension (first three rows for each haplogroup), along with Spearman's ρ for the Mantel test (with associated P value), for haplogroups M (without M16), O, P (including P4b1 and P5 separately) and S, and the pooled samples (All). Analyses were performed on the 76 samples with reliable provenance (see Methods and Supplementary Table 3).